Cohesive Self-Gravitating Aggregates and their Path of Disruption Paul Sánchez and Daniel J. Scheeres, Colorado Center for Astrodynamics Research, University of Colorado, Boulder, CO 80309-431 (diego.sanchez-lana@colorado.edu)

We simulate the failure mechanics of cohesive and cohesionless, spherical and ellipsoidal self-gravitating aggregates in order to better understand the geophysics of rubble pile asteroids. The aggregates are slowly spun up to disruption controlling for angle of friction, cohesion and global shape. In particular we observe whether these bodies fail by shedding or fission and find a clear transition from one to the other as a function of geophysical properties.

Introduction:

During the last few years different researchers have used DEM codes for the simulation of small rubble pile bodies. This research has pushed code developers to implement different models to simulate frictional and cohesive forces. This however, has led to different paths for the disruption of self-gravitating aggregates depending on the researcher and even the code that has been used. Notice that we have not used the term asteroid as an equivalent to the simulated aggregates. We have done this intentionally, though images can and do resemble real asteroids, the fact is that the outcomes of a simulation, and how real they are, depend on how well said simulations capture the physics of the real system.

In this paper we take two parameters, angle of friction (θ) and cohesive strength (σ_c), and explore their effect on the disruption process of aggregates with different initial shapes. We have chosen to use spherical and ellipsoidal shapes as the starting point of the evolution as these are classical forms that could also be studied analytically.

Simulation Method:

The simulation program that is used for this research applies a Soft-Sphere Discrete Element Method [1, 2, 3, 4] to simulate a self-gravitating granular aggregate. The particles, modelled as spheres that follow a predetermined size distribution, interact through a soft-repulsive potential when in contact. This method considers that two particles are in contact when they overlap. When this happens, normal and tangential contact forces are calculated ([5]).

The calculation of the normal forces between colliding particles is modeled by a linear spring and a dashpot. The elastic force is modelled as

$$\vec{\mathbf{f}}_e = k_n \xi \hat{\mathbf{n}}, \tag{1}$$

the damping force as:

$$\vec{\mathbf{f}}_d = -\gamma_n \dot{\xi} \hat{\mathbf{n}}, \tag{2}$$

and the cohesive force (f_c) between the particles is calculated as a function of the (not simulated) interstitial regolith [6] and the size of the simulated particles. Scaling arguments allow us to regard simulations with the same aggregate size and different σ_c as equivalent to simulations of aggregates of different size and the same σ_c.

Then the total normal force is calculated as $\vec{\mathbf{f}}_n = \vec{\mathbf{f}}_e + \vec{\mathbf{f}}_c + \vec{\mathbf{f}}_d$. In these equations k_n is the elastic constant, ξ is the overlap of the particles, γ_n is the damping constant (related to the dashpot), $\dot{\xi}$ is the rate of deformation and $\hat{\mathbf{n}}$ is the vector joining the centres of the colliding particles. This dashpot models the energy dissipation that occurs during a real collision.

The tangential component of the contact force models surface friction, static and dynamic. This is calculated by placing a linear spring at the contact point, attached to both particles, at the beginning of the collision [5, 7], producing a restoring frictional force $\vec{\mathbf{f}}_t$. The magnitude of the elongation of this tangential spring is truncated in order to satisfy the local Coulomb yield criterion $|\vec{\mathbf{f}}_t| \leq \mu|\vec{\mathbf{f}}_n|$. In addition, we have also implemented rolling friction as suggested by [8]. For this, a winding spring provides a torque to particles in contact. In form, it is very similar to surface friction, but is related to the relative angular displacement. This type of friction allows us to obtain aggregates with angles of friction of up to ~35°, typical of cohesionless aggregates on Earth, though angles of ~40° are not rare.

The particles (initially cohesionless and frictionless) are left to coalesce in the desired shape so forming very homogeneous internal structures. The aggregates are spun up in small, discrete increments around their CM and the disruption process is observed.

Results:

For our simulations we have chosen the following angles of friction: 12°, 25° and 35°. These values were calculated using the Drucker-Prager yield criteria [9] and represent only the lower bound of the envelope for cohesionless aggregates.

We first show the disruption mode of cohesionless aggregates. Fig. 1 shows the disruption of spherical (top) and ellipsoidal (bottom) aggregates with increasingly higher angles of friction from left to right. For θ=12°, the initially spherical aggregate deforms first to an oblate and then to a prolate spheroid, finally shedding some particles. No surface friction was included in these simulations so this is in fact a granular liquid. For θ=25°, the deformation stops when an oblate

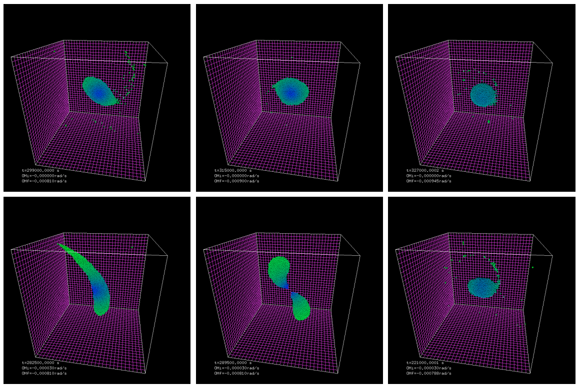

Figure 1: Deformation and disruption of three initially spherical (top) and three ellipsoidal (bottom) non cohesive aggregates.

shape has been reached and then there is some material shedding from the equatorial ridge. For θ=35°, there is also deformation towards an oblate spheroid, but to a lesser degree and the mass shedding is not particle by particles, but in groups of a few.

The deformation of the ellipsoidal aggregates follow a different pattern. For θ=12°, the aggregate simply deforms into something that could be seen as extreme shedding. For θ=25°, the aggregate has some more structural strength as surface-surface friction has been included. Deformation occurs at the centre, the place where greater stress is located. For θ=35°, the aggregate deforms very little and shedding particles from one end is preferred to fission. As in the spherical case, shedding occurs in groups of a few particles.

In both cases, the inclusion of extra sources of friction at the particle level translate into greater structural strentgh, less deformation and a greater angle of friction. This is how all these aggregates are related, if the body is strong enough to resist deformation, the spin-ups can continue until at some point the particles at the farthest ends can get into orbit. Of course, how the deformation occurs depends on the initial shape. Prolate spheroids cannot go towards spherical or oblate shapes, but the opposite direction is possible.

Fig. 2 shows the deformation and disruption of three initially spherical aggregates (top) and three initially ellipsoidal aggregates (bottom) with increasing cohesive strength from left to right. All of them have a friction angle θ of at least at 35°. From these images we see that as cohesion is increased the nature of the body distortion and deformation changes. For low cohesion the body tends to shed chunks of material from its surface, while for increasing cohesion the body undergoes larger deformations that lead to the fission of significant components of the body. If, instead, we assume that the cohesion is constant for these bodies but

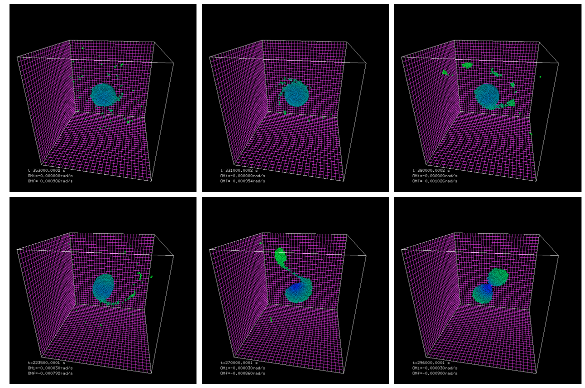

Figure 2: Deformation and disruption of three initially spherical (top) and three ellipsoidal (bottom). From left to right the aggregates have greater cohesive strength (or same strength and diminishing size)

that their size is scaled, the aggregates measure about 1 km, 3 km and 14 km across and the particles, or groups of particles, have a similar size, making this a problem of resolution, i.e., the number of particles used in a simulation.

These results start to raise fundamental questions regarding the difference between shedding and fission. Is it shedding when it is dust grain by dust grain ejection from the main body or when it is in groups of 10, 100 or 100000 dust particles? Is it fission when a 1 m piece of the asteroid detaches or when it splits in the middle? These questions will be further pursued in the conference presentation.

References: [1] P. Sánchez, et al. (2011) *The Astrophysical Journal* 727(2):120. [2] P. Cundall (1971) in *Proceedings of the International Symposium on Rock Mechanics* vol. 1 129–136 -, Nancy. [3] P. A. Cundall, et al. (1992) *Engineering Computations* 9(2):101 `doi`. [4] M. P. Allen, et al. (1989) *Computer Simulation of Liquids* Oxford science publications Oxford University Press, USA, New York ISBN 0198556454. [5] H. Herrmann, et al. (1998) *Continuum Mechanics and Thermodynamics* 10:189 ISSN 0935-1175 10.1007/s001610050089. [6] P. Sánchez and Daniel J. Scheeres (2012) The Strength of Regolith and Rubble Pile Asteroids, submitted and available on ArXiv. [7] L. E. Silbert, et al. (2001) *Phys Rev E* 64(5):051302 `doi`. [8] J. Ai, et al. (2011) *Powder Technology* 206(3):269 ISSN 0032-5910 `doi`. [9] D. P. Sánchez, et al. (2012) *Icarus* 218(2):876 ISSN 0019-1035 `doi`.